IEEE Access
Multidisciplinary | Rapid Review | Open Access Journal

Received 22 September 2023, accepted 5 October 2023, date of publication 12 October 2023, date of current version 19 October 2023.

Digital Object Identifier 10.1109/ACCESS.2023.3324078

RESEARCH ARTICLE

FRA-Based Parameter Estimation for Fault Diagnosis of Three-Phase Voltage-Source Inverters

YU LUO[1], LI ZHANG[2], (Senior Member, IEEE), CHUNYANG CHEN[1], KANG LI[2], (Senior Member, IEEE), TIANJIAN YU[1], AND KAIDI LI[3]

[1]School of Traffic and Transportation Engineering, Central South University, Changsha 410075, China
[2]School of Electrical Engineering, University of Leeds, LS2 9JT Leeds, U.K.
[3]Shenzhen Metro Group, Shenzhen 518000, China

Corresponding author: Kaidi Li (likaidi@shenzhenmc.com)

This work was supported by the Fundamental Research Funds for the Central Universities of Central South University under Grant 2018zzts164.

ABSTRACT This paper presents a fault detection and location identification method for single and double switch Open Circuit Fault (OCF) in three phase voltage source inverters (VSIs) based on current model parameter estimation. The proposed method requires the measurement of the inverter currents to build a dynamic model. A fast recursive algorithm (FRA) is used to estimate the model parameters under either normal and various fault conditions, hence generating a set of fault diagnosis vectors (FDVs) which form a base matrix. A simplified K-Nearest Neighbour (KNN) algorithm is designed to detect the nearest distance, in this case, the Manhattan distance, between the monitored FDV to the normal FDV. When an open-circuit fault occurs, the distance between the two will be significantly increased than a set threshold, hence the fault occurrence can be effectively detected. A simple and effective function based on the analysis of the identified FDV and those in the base matrix is designed to locate the faulty switches. Experimental results under different fault cases are presented to confirm the effectiveness of the method.

INDEX TERMS Voltage source inverter, open circuit fault, fault diagnosis, parameter estimation.

I. INTRODUCTION

Three-Phase voltage-source inverters (VSIs) are widely used in industry for their high efficiency and control flexibility. Inverters convert power from DC sources, such as batteries, solar cells or fuel cells, to AC voltages at varied frequencies and magnitudes. They are crucial in a wide range of applications such as pumps, fans, compressors, electric vehicles, and railway traction drives. etc. VSIs are also widely used in power systems for interfacing renewable sourced generators such as photovoltaic or wind farms to grids, or compensating reactive power as power conditioners. All these applications are subject to many types of faults, of which those due to VSIs are most commonly due to power semiconductor switch devices which are relatively fragile and highly stressed electrically. Inverters in motor drives are used to adjust the speeds of AC motors [1], [2], by varying frequencies and waveforms according to command AC voltages. Power switches used are mostly Metal Oxide Semiconductor Field Effect Transistors (MOSFETs) and Insulated Gate Bipolar Transistors (IGBTs) [3], [4]. More recently, technological advances in the manufacture of power devices based on wide bandgap materials, such as silicon carbide (SiC) or gallium nitride (GaN), have led to their applications in inverters [5]. Power switches become faulty due to ageing, overloading or unpredictable operating conditions and are the most vulnerable components in inverters [6]. Switches in three-phase VSIs can suffer from short-circuit and open-circuit faults. The short-circuit fault is destructive; it causes a high current flow, and, in most cases, is detected by the standard protection system, such as fuses and circuit breakers, and makes the inverter shutdown immediately [7].

The associate editor coordinating the review of this manuscript and approving it for publication was Francisco Perez-Pinal.

Unlike short-circuit fault protection, open-circuit fault (OCF) protection is generally not included as a standard feature in industrial applications, but open-circuit faults also cause drive malfunctions and could lead to secondary faults in other components of a drive system [8], [9]. It is therefore important to develop fast and accurate switch open-circuit fault diagnosis methods to prevent faults from propagating to other parts of the system. Open-circuit diagnosis is also essential for ensuring stable operation of inverters as it avoids prolonged operation with a faulty switch, which causes output current and voltage waveform distortion, abnormal load operation, overheating and so on [10], [11].

At the present, OCF diagnosis methods can be classified into four categories; the conventional voltage/current-based approaches, signal processing-based methods, model-based and artificial intelligence (AI) technology methods. The conventional methods, such as those rely on either voltage and current measurements, have been extensively explored. Those methods based on measured voltages proposed in [12], [13], [14], [15], and [16] discover the faults by comparing the actual measured phase or line voltages with the corresponding command voltages. The approach is simple and generally shows good performance and high detection speed, but requires extra voltage sensors and associated diagnostic circuits. Current-based methods, on the other hand, eliminate the need for additional sensors, and hence save space and cost. In particular the conventional current-based methods relying on direct analysis of load currents have been widely applied in fault diagnosis of three-phase VSI systems. In [17], a diagnostic variable is set by using phase current summed with its corresponding semi-periodic phase-difference counterpart and subsequently normalizing the result by dividing the periodic absolute value of the phase current. The computation process is simple and result concise, however it needs to apply a variable parameter moving average method to improve the diagnostic speed. In addition it requires using an auxiliary diagnostic variable for the special cases of double simultaneous faults in the same phase which may incur inaccurate results. In [18], a normalized phase current based on Park's transformation is used to calculate the average value; it reflects the symmetry feature of the detected signals. In general phase-current-based methods are sensitive to load regulation and setting an appropriate threshold for fault identification can be an issue. They may misdiagnose the faults when load currents change rapidly, and hence some optimization methods have been proposed. In [19] the zero sequence current based method is proposed which overcomes the load regulation effects. The disadvantage of this approach is that there are some limitations in identifying the fault locations of an inverter, it needs the mutual interference to locate the faults according to the circuit topologies. In [20] the proposed method can detect any faults under any circumstances and identify the origin of them. However, this method does not perform well in response to load changes and can not deal with the three-phase inverter system under complex working conditions. A method which simplifies the calculation is based on monitoring sustained near-zero output current. This improves the reliability of the diagnosis [21], [22], but it is only applicable to three-phase inverters under certain operating conditions.

Signal processing-based methods have also been applied the detection and diagnosis of OCFs in voltage source inverters. In particular wavelet transform(WT) in the frequency domain analysis has been used. In [23], WT is applied to analyze inverter phase current waveform first, the integrals of the derived WT coefficients over several cycles, named as the total energy of each coefficient, are used to identify the fault features, and changes in these help to pinpoint the faulty switch. However, the changes of the load and torque significantly influence the accuracy of diagnosis. In [24], the wavelet packet transform is applied to extract a distinguishable electromagnetic signature, but a primary limitation of the developed diagnostic methodology is that its applicability is exclusively to motor drives. Electromagnetic signatures can be used to detect OCFs, relying on semiconductor device interferences. In [25] and [26], authors added Electromagnetic Interference (EMI) filters at the inverter's output. These filters measure voltages across resistors and compare them to the expected values when without faults, hence helping to locate open switch faults. However, in some cases, EMI signatures can be too similar to distinguish the fault switch location. To address this, a complex combination of time domain signals, and multi-scale wavelet analysis is used for obtaining a higher accuracy. It is worth noting that adding EMI filters increases system costs.

In recent years, model-based fault diagnosis for inverter drive systems has been widely researched. In [27], a fast diagnosis method for OCFs in inverters without sensors is studied by analysing the switching function model of the inverter under both normal and faulty conditions, because the faulty information is extracted from the switch voltages, the robust performance of the method is in question. In [28], a current residual vector-based fault diagnosis method is presented to eliminate the effects of the load. This method can quickly and effectively detect the fault of the inverter, but is not able to identify the location of the faulty switch. In [13] and [29], a simple method for single and double switch OCF diagnosis based on three-phase current distortions in VSIs for vector controlled induction motor drives is studied. The method depends on the determination of the rotation angle of the current vector, which is affected by the noises and complexity of system.

In the realm of artificial intelligence (AI) technology, various algorithms have been researched and developed for the classification of OCFs in inverters. In [30], the authors utilized the Self-Organizing Map (SOM) method for OCFs detection and showed the simplicity of the method together with its straightforward training process. However, the accuracy diminishes when it is applied to complex and nonlinear systems. In [31], a Grey Wolf Optimization Support

Vector Machine (GWO-SVM) is introduced for fault diagnosis in three-phase inverters used with permanent magnet synchronous motors. While this algorithm offers advantages such as reduced training time, lower computational complexity, and faster implementation and testing, it exhibits lower efficiency in complex applications. In [32], a probability principal component analysis-support vector machine (PPCA-SVM) was employed as a fault diagnosis tool in both simulations and experiments, delivering highly reliable fault diagnosis for cascaded H-bridge multi-level inverters. Nevertheless, additional research is required to adapt this method for complex scenarios. In [33], a novel 1-D Convolutional Neural Network (CNN) with an improved stochastic gradient optimization method is presented for precise and speedy fault diagnosis in three-level Neutral Point Clamped (NPC) inverters. It performs well in terms of both speed and accuracy, but it requires a substantial amount of corresponding inverter fault data for training to maintain effectiveness.

Most of the aforementioned approaches are complicated and computationally costly for real-time application. This paper presents a simple, low-cost, model parameter-based method for OCF diagnosis of a three-phase VSI in real time. Using a discrete-time current model of a VSI system, the parameters of this model can be estimated using the Fast Recursive Algorithm(FRA) [34]. These parameters exhibit characteristics of different types of open-circuit faults, hence they form the fault diagnosis vectors (FDVs). A simple calculation function is developed which uses the FDVs to identify the fault appearance and locate the fault switch in a three-phase inverter. Compared with the existing methods, the distinctive feature of the proposed method are evident on several aspects; it is more sensitive to detect a fault and accurate in locating its location and has the feature of fast diagnosis speed compared with the conventional current diagnosis method. It can evaluate the parameters in real time and requires no additional hardware on top of that already used for normal operation. The method has a wide range of applications, including traction drive systems in addition to general machine drive systems.

The rest of this paper is organized as follows. Section II focuses on inverter topology and fault currents, different fault cases are described and analyzed. Then, the parameters model based on α-β currents and estimation algorithm are proposed in Section III. The diagnosis method based on the parameters estimation model is illustrated and the fault detection and location functions are introduced in section IV. Consequently, the experimental platform is introduced to validate the proposed diagnosis approach, and the experimental results show the validity and feasibility of the proposed method in section V. Finally, conclusions are given in section VI.

II. THREE-PHASE VSI AND FAULT ANALYSIS

A. THREE PHASE VSI

Fig. 1 illustrates a typical three-phase voltage source inverter with six identical switches T_1-T_6. There are also devices D_1-D_6 which are anti-parallel diodes associated to each switching device. Gate signals g_1-g_6 control the ON and OFF state of T_1-T_6. When gate signal is 1, the corresponding switch conducts, and when it is 0, the switch turns off. The gate signals for two switches on one phase leg are complementary. Sinusoidal pulse width modulation(SPWM) is a common technique to generate the gate signals. A VSI may supply a three-phase R-L load or an ac machine and a three-phase L-C filter is commonly connected at its output terminals for suppressing high order harmonics due to switching as shown in Fig. 1. For ease of analysis and assuming balanced operation such a load circuit can be simplified to a per phase equivalent R-L-C circuit as shown in Fig. 2.

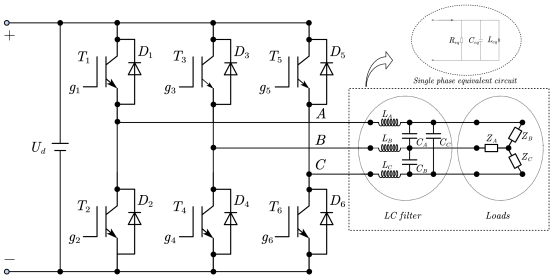

FIGURE 1. Topology of three phase inverter.

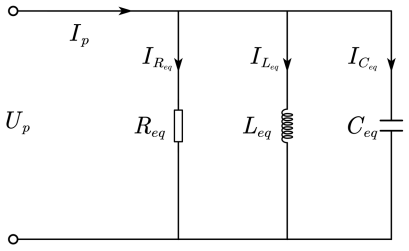

FIGURE 2. Equivalent load circuit for each phase.

Under healthy condition, the three phase output currents are the sinewaves with equal amplitude, and 120° phase difference between them and expressed as

$$i_p(t) = I_m \sin\left(\omega t + \Phi_p\right) \tag{1}$$

where p = a, b, c stands for different phases. I_m is peak phase current, ω denotes current angular frequency, Φ_p is the phase angle with the reference axis and Φ_a=0, Φ_b=$-2\pi/3$, Φ_c=$-4\pi/3$.

Considering R-L-C load circuit in Fig. 2, the voltage U_p and current I_p should be equal to those of the inverter circuit in Fig. 1. According to the Kirchhoff's current law, the per phase current can be defined as

$$i_p = \frac{u_p}{R} + \int \frac{u_p}{\omega L} dt + \frac{1}{\omega C}\frac{du_p}{dt} \tag{2}$$

B. FAULT CURRENT ANALYSIS

In three-phase VSIs, single switch or double switches open-circuit faults are most common in practice. Table 1

TABLE 1. Fault classification and labels.

Case	Faulty switch	Label	Case	Faulty switch	Label
Nomal	No fault	0	III	T_1, T_4	11
I	T_1	1		T_1, T_5	12
	T_2	2		T_1, T_6	13
	T_3	3		T_2, T_3	14
	T_4	4		T_2, T_4	15
	T_5	5		T_2, T_5	16
	T_6	6		T_2, T_6	17
II	T_1, T_2	7		T_3, T_5	18
	T_3, T_4	8		T_3, T_6	19
	T_5, T_6	9		T_4, T_5	20
III	T_1, T_3	10		T_4, T_6	21

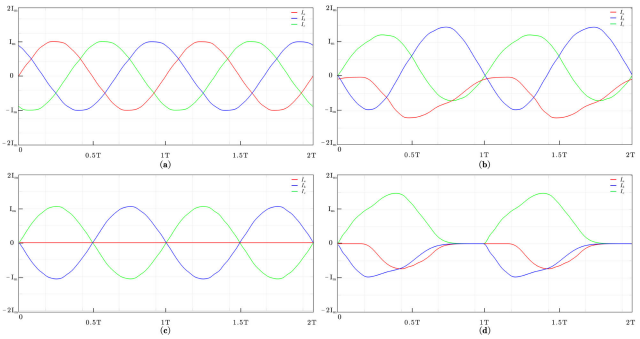

FIGURE 3. Currents of each phase. (a) nomal state. (b)OCF in T_1. (c) OCFs in T_1 and T_2. (d) OCFs in T_1 and T_3.

shows 22 types of inverter operation conditions. It includes the normal working condition and 21 fault conditions. The fault conditions are divided into three categories and each fault is assigned to a different number as a label. The cases stand for different fault classifications. Case I: Single OCF. Case II: Two OCFs in the same inverter leg. Case III: Two OCFs in two different inverter legs.

Fig. 3 shows the phase current waveforms of an inverter under four different conditions. Under healthy condition, the three-phase currents are well-balanced sinusoidal waves with phase shift of 120 degrees between each other. When a single switch OCF occurs, the current through the phase where the OCF occurs is distorted and uni-polar, and three-phase currents become unbalanced. When the two OCFs occur in the same inverter phase leg, the current of the faulty phase becomes 0, while the currents through other two phases become anti-phased with equal magnitude. When the heterogeneous double switch OCFs arises, the two OCFs appeal in two different inverter phase legs, all three phase currents are distorted, and two become uni-polar as shown in Fig. 3(d).

To simplify the analysis, three phase currents can be transformed to their equivalent i_α and i_β elements in α-β axes using Clarke transformation, the equation is defined as

$$\begin{bmatrix} i_\alpha \\ i_\beta \\ i_0 \end{bmatrix} = \frac{2}{3} \begin{bmatrix} 1 & -\frac{1}{2} & -\frac{1}{2} \\ 0 & \frac{\sqrt{3}}{2} & -\frac{\sqrt{3}}{2} \\ \frac{1}{2} & \frac{1}{2} & \frac{1}{2} \end{bmatrix} \begin{bmatrix} i_a \\ i_b \\ i_c \end{bmatrix} \tag{3}$$

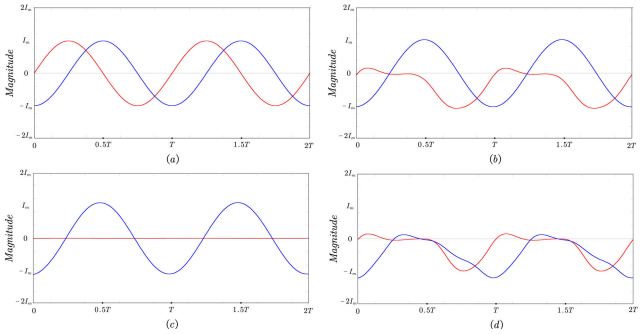

FIGURE 4. α-β axis currents under different condition. (a) nomal state. (b) OCF in T_1. (c) OCFs in T_1 and T_2. (d) OCFs in T_1 and T_3.

Under different conditions i_α and i_β of VSI have their own distinctive features and are different from each other. i_α and i_β in normal condition and other three OCF states are shown in Fig. 4. In normal state, the waveforms of α-β currents are sinusoidal and balanced with 90 degree phase difference. However, when OCFs happen, each OCF state generates a distinctly different current pattern as can be seen in Fig. 3(b)-(d). Though the frequencies of the two current elements remain unchanged but their magnitudes and average values are totally different. In this work α-β currents are used for the fault diagnosis.

III. PARAMETERS ESTIMATION

A. CURRENT MODEL AND PARAMETERS

According to Equations (2) and (3), under normal condition, the relationship between α-β voltages and currents can be expressed as

$$i_{\alpha\beta} = \frac{u_{\alpha\beta}}{R} + \int \frac{u_{\alpha\beta}}{\omega L} dt + \frac{1}{\omega C} \frac{du_{\alpha\beta}}{dt} \tag{4}$$

Assuming sample time T_S is significantly small compared to the load currents period time, the discrete time expression of this formula at time instant k is

$$\begin{aligned} \frac{i_{\alpha\beta}(k) - i_{\alpha\beta}(k-1)}{T_S} &= \frac{u_{\alpha\beta}(k) - u_{\alpha\beta}(k-1)}{T_S} \\ &+ \frac{u_{\alpha\beta}(k)}{\omega L} + \frac{1}{\omega C} \\ &\times \frac{u_{\alpha\beta}(k) - 2u_{\alpha\beta}(k-1) + u_{\alpha\beta}(k-2)}{T^2{}_S} \end{aligned} \tag{5}$$

The above equation can be simplified as

$$\begin{aligned} i_{\alpha\beta} - i_{\alpha\beta}(k-1) &= Au_{\alpha\beta}(k) \\ &+ Bu_{\alpha\beta}(k-1) + Cu_{\alpha\beta}(k-2) \end{aligned} \tag{6}$$

where A, B, C are model parameters expressed as

$$A = \frac{1}{R} + \frac{1}{\omega C T_S} + \frac{T_S}{\omega L} \tag{7}$$

$$B = -\frac{2}{\omega C T_S} \tag{8}$$

$$C = \frac{1}{\omega C T_S} \tag{9}$$

Thus, for a three-phase inverter, a linear relationship between its current and voltage under normal condition at the kth time instant can be written as

$$Y(k) = \left[u_{\alpha\beta}\ u_{\alpha\beta}\ (k-1)\ \ u_{\alpha\beta}\ (k-2)\right] \begin{bmatrix} A \\ B \\ C \end{bmatrix} + \varepsilon\ (k) \tag{10}$$

where $Y(k) = i_{\alpha\beta}\ (k) - i_{\alpha\beta}\ (k-1)$ and ε (k) is the model mismatched disturbance, and it is a bounded disturbance with a very small value, making it negligible. The parameters A, B, C of the system can be evaluated by an algorithm, named the fast recursive algorithm (FRA), its principle and application to the inverter model parameter estimation are discussed as follows.

B. CURRENT MODEL AND PARAMETERS

In the system identification field, there are the possibilities that models identified can have excessive number of parameters which may lead to over-fitting and enormous computational burden. The fast recursive algorithm is featured by identifying only the dominant parameters in a nonlinear dynamic system using linear-in-the-parameter model. FRA can both select the model structure and estimate the model parameters. Its merit lies in that it requires much less computational effort and also numerically more stable than orthogonal least squares approach which is a common method used in linear parameter identification. Consider a nonlinear discrete-time dynamic system with N input and output data samples $\{\boldsymbol{x}\ (i)\ , y\ (i)\}_{i=1}^{N}$ and have the expression given as

$$\mathbf{y} = \Phi\Theta + \Xi \tag{11}$$

where the system output $\Phi = [\varphi\ (1)\ , \ldots, \varphi\ (j)\ , \ldots \varphi\ (N)]^T \in \Re^{N\times S}$ is the regression matrix that contains all parameter terms, each term $\varphi\ (j) \in \Re^{N\times 1}$ represents a nonlinear function of N input samples $\varphi\ (j) = \left[\varphi_j\ (x\ (1))\ , \ldots, \varphi_j\ (x\ (N))\right]^T$ $(j = 1, \ldots, S)$ are the unknown parameters to be identified, and $\Theta = [\theta_1, \ldots, \theta_s]$ is the model residual vector. Two recursive matrixes $\mathbf{M}_k$ and $\mathbf{R}_k$ are predefined in FRA to fulfill the forward model selection procedure as

$$\mathbf{M_k} = \Psi_k^T \Psi_k \tag{12}$$

$$\mathbf{R_k} = \mathbf{I} - \Psi_k^T \mathbf{M}_k^{-1} \Psi_k \tag{13}$$

where $\Psi_k \in \Re^{N\times k}$ includes the first k columns of the full regression matrix Ψ, additionally, k=1,…,S, and $\mathbf{R}_0 =$ I. Thus, when the first k columns in Φ are selected, the estimation of parameters that minimizes the cost function and the associated minimal cost function can be formulated as

$$\hat{\Theta}_k = \mathbf{M}_k^{-1} \Psi_k \mathbf{y} \tag{14}$$

$$E_k = \mathbf{y}^T\mathbf{y} - \hat{\Theta}_k^T \psi_k^T \mathbf{y} = \mathbf{y}^T\mathbf{y} \tag{15}$$

To simplify the formulas and decrease the computational complexity, three quantities are consequently defined as

$$\varphi_j^{(k)} \triangleq \mathbf{R}_k \varphi_j,\ \varphi_j^{(0)} \triangleq \mathbf{R}_0 \varphi_j = \varphi_j \tag{16}$$

$$a_{k,j} \triangleq \left(\varphi_k^{k-1}\right)^T \varphi_j^{(k-1)},\ a_{1,j} \triangleq \varphi_1^T \varphi_j \tag{17}$$

$$b_k \triangleq \left(\varphi_k^{k-1}\right) y,\ b_1 \triangleq \left(\varphi_1^0\right)^T y = \varphi_1^T y \tag{18}$$

where j=1,…,S, and k=1,…,S. According to the properties of $\mathbf{R}_k$, the net contribution of a new model term φ_{k+1} to the cost function can be explicitly calculated as

$$\begin{aligned} \triangle E_{k+1} &= -\frac{\left(y^T \varphi_{k+1}^k\right)^2}{\left(\left(\varphi_{k+1}^{(k)}\right)^T \varphi_{k+1}^{(k)}\right)} \\ &= \frac{\left(b_{k+1}^T\right)}{a_{k+1,k+1}}, k = 0, 1, \ldots, S-1 \end{aligned} \tag{19}$$

By calculating the net contribution of each term, the model terms with maximum contributions will be selected one by one. Finally, after all important model terms have been selected, the parameter for each selected term is calculated as

$$\hat{\theta}_j = \frac{b_j - \Sigma_{i=j+1}^{k} \hat{\theta}_j a_{j,i}}{a_{j,i}}, j = k, k-1, \ldots, 1 \tag{20}$$

Equations (14) and (15) constitute the main steps of the FRA, which selects model terms one by one based on (19) and calculates the model parameters for the resultant model based on (20).

C. MODEL PARAMETER ESTIMATION BY FRA

Load variations change α-β currents, hence affect estimated parameter values. To eliminate this influence, the values of the measured α-β currents need to be normalized after the Clarke transformation. The normalization formula is as follows

$$U_{norm} = U_{ref}/U_{\alpha\beta m} \tag{21}$$

$$I_{norm} = I_{ref}/I_{\alpha\beta m} \tag{22}$$

where U_{norm}, I_{norm} is the normalized value. $U_{\alpha\beta m}$ and $I_{\alpha\beta m}$ are the amplitude of the α-β voltages and currents under normal rated condition. Applying FRA for parameter estimation, the first step establishes the output and input data vectors given by (10) using sampled data as

$$y = i_{\alpha\beta}\ (k) - i_{\alpha\beta}\ (k-1) \tag{23}$$

$$\Phi = \left[u_{\alpha\beta}\ u_{\alpha\beta}\ (k-1)\ \ u_{\alpha\beta}\ (k-2)\right] \tag{24}$$

Then the linear formula (11) can be formed with vector containing the parameters A, B, and C to be estimated. These

are evaluated by applying formula (20). The contribution of the acquired parameters to the linear system's error can be calculated by (19).

The detailed procedure for identifying the parameters of the three-phase inverter by means of FRA is as follows:

1)The sampled current signal of the inverter and the corresponding reference voltage signal are fed into (11) for estimating model parameters by formula (20).

2) For accurate and fast fault tracking in real-time, a moving data window with a time width of a half-sinusoidal cycle is used for data logging.

3) The current and voltage samples are logged into this data window by first-in and first-out (FIFO) when it is filled, while FRA uses updated data set to perform parameter estimation at each sample step. Thus real-time monitoring of the inverter parameters is achieved.

IV. FAULT DIAGNOSIS BY ESTIMATED PARAMETER VECTORS

A. FAULT DIAGNOSIS VECTORS

Consider all operation cases listed in Table 1, each corresponds to a unique model parameter set, by aggregating the parameter sets for all these cases, a database can be formed which can be used for fault identification. The proposed fault diagnosis scheme builds such a database by taking a three-phase inverter drive as a black box and simulating it under all operation conditions. The input of the black box is the three-phase voltage which are the inverter reference voltage U_{ref} with known constant amplitude and phase angles under the normal case. The output of the black box is the measured current signals. Both input and output signals are sampled and then transformed to their equivalent α-β values using Clark transformation. For both α and β currents two model equations (Equ(6)) are derived, and they have in total six model parameters, (A_α, B_α, C_α, A_β, B_β, C_β) forming a vector with 6 elements. Applying FRA, all the elements in a vector can be estimated. For different fault cases listed in Table 1, the estimated vectors are different representing the characteristic feature of each case. This fact enables fault diagnosis and location identification be performed accurately. so the parameter vector is named the fault diagnosis vector (FDV) defined as

$$\text{FDV} \triangleq \left[A_\alpha \; B_\alpha \; C_\alpha \; A_\beta \; B_\beta \; C_\beta\right]^T \tag{25}$$

Since there are 22 different operation states including normal one, 22 FDVs are derived to cover the inverter for all operation states, they form a base matrix written as

$$\text{FDV}_{basei} \triangleq \left[A_{\alpha i} \; B_{\alpha i} \; C_{\alpha i} \; A_{\beta i} \; B_{\beta i} \; C_{\beta i}\right]^T \tag{26}$$

where i = 0-21, stands for all 22 parameter sets for inverter at normal and OCF conditions. This base matrix is the most crucial for the fault detection and location identification of the inverter OCFs.

Fig. 5 summarizes the procedure for estimating the parameter vectors of a three-phase VSI model. It includes

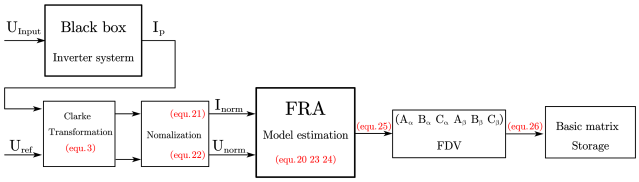

FIGURE 5. Procedure for fault diagnosis vector derivation.

current and voltage sampling, their transformation to α-β elements(Equ(3)) and normalization (Equ (21,22)), then combining them to build the linear model (Equ (23,24)), the parameters can be obtained by equation(20). Subsequently FRA is applied to derive the parameter set of the inverter corresponding to the set cases. The above process is repeated for deriving FDVs of all possible fault cases (Equ (25,26)), the resultant FDVs are stored to form a base matrix which is used for fault detection of the corresponding inverter drive system.

B. FAULT DIAGNOSIS BY SIMPLIFIED KNN ALGORITHM

The K-Nearest Neighbour (KNN) algorithm is a simple but effective classification method that utilizes proximity to make predictions about grouping a dataset around a point [35]. Specifically, it is a method that uses a training dataset of k samples to classify new input instances. When faced with a new input instance, the algorithm identifies the K closest instances in the training dataset using a distance metric of choice. It then assigns the input instance to the class that is most frequently represented among these K nearest neighbors.

This paper describes an approach to detecting faults in inverters using a simplified K-Nearest Neighbors (KNN) algorithm. To streamline the approach, the K value is set to 1, resulting in a training set that consists of only one sample. This streamlined approach allows us to focus on the most critical distinctions in the data, while still achieving accurate and reliable fault detection.

The distance in the KNN (K-Nearest Neighbors) algorithm is a metric used to calculate the similarity or distance between samples. Let x and y be n-dimensional vectors in the real vector space R^n, the distance between x and y is defined as follows:

$$L_p\left(x, y\right) = \left(\sum_{i=1}^{n} |x_i - y_i|^p\right)^{\frac{1}{p}} \tag{27}$$

When p = 2, it is the Euclidean distance, and when p=1, it is the Manhattan distance. A higher value of parameter p requires more computational power. Due to the significant distinctions among the FDVs corresponding to each VSI condition, in this paper, we assess and measure classification using the Manhattan distance, which requires the least computation and is also competent for the task. The formula

for the Manhattan distance is as follows.

$$L_1(x, y) = \sum_{i=1}^{n} |x_i - y_i| \tag{28}$$

With base matrix established, each FDV in it corresponds to a unique faulty state, one can distinguish them by evaluating Manhattan distance. Applying this to FDVs in the base matrix, the Manhattan distance between two FDVs can be calculated as V_{Man}.

$$V_{Man} = L_1(\text{FDV}_{est} - \text{FDV}_{normal}) \tag{29}$$

where the FDV_{est} is the estimated FDV of the system and the FDV_{normal} is the parameter vector of the normal condition.

During normal operation under different loads, the inverter current waveforms change only in magnitude, the corresponding parameter vector does not change much. So V_{Man} should ideally be small. However if V_{Man} is large, it indicates a fault is present. Thus the occurrence of an OCF is detected as

$$F_{detection} = \begin{cases} 1 & if \ K * V_{Man} \geqslant 1 \\ 0 & if \ K * V_{Man} < 1 \end{cases} \tag{30}$$

where K is a parameter used to make it easier to observe V_{Man} values. In this paper, it is set to 10. By multiplying this parameter, one can determine whether a fault has occurred by checking whether the Manhattan distance exceeds the critical value of 1. If the $F_{detection} = 1$, it indicates that an OCF happens in the inverter. If the $F_{detection} = 0$, inverter is operating under normal condition.

Once the existence of an OCF in confirmed through the above process, identification of fault location or fault state out of 21 listed in Table 1 is followed. This is performed by comparing the estimated FDV with all other 21 fault parameter vectors in the base matrix (26) and equation (31) is gained and applied.

$$V_{Mani} = L_1(\text{FDV}_{est} - \text{FDV}_{basei})_{i=1\ 21} \tag{31}$$

The V_{Mani} giving the lowest value gives the OCF identified and is assigned to the corresponding fault label number. In this case the fault location function is defined as

$$F_{location} = \min\{V_{Mani}\}_{i=1-21} \tag{32}$$

Fig. 6 displays the flowchart of the three-phase VSI OCF diagnosis process which is also summarized below.

1) The first step is to obtain the FDV_{est} of the three-phase inverter real-time system via FRA estimation, the detailed procedure for the FDV generation has been provided in fig. 5.

2) The next step is to use the FDV_{est} to perform a fault diagnosis on the three-phase VSI. The Manhattan distance between the FDV_{est} and the FDV_{nomal} is calculated (Equ (29)) and the V_{Man} is substituted into the fault detection function $F_{detection}$ (Equ (30)) to detecte the occurrence of a fault. If $F_{detection} = 0$, no faults occur and system monitoring continues. If $F_{detection} = 1$, a fault has occurred and fault location is required.

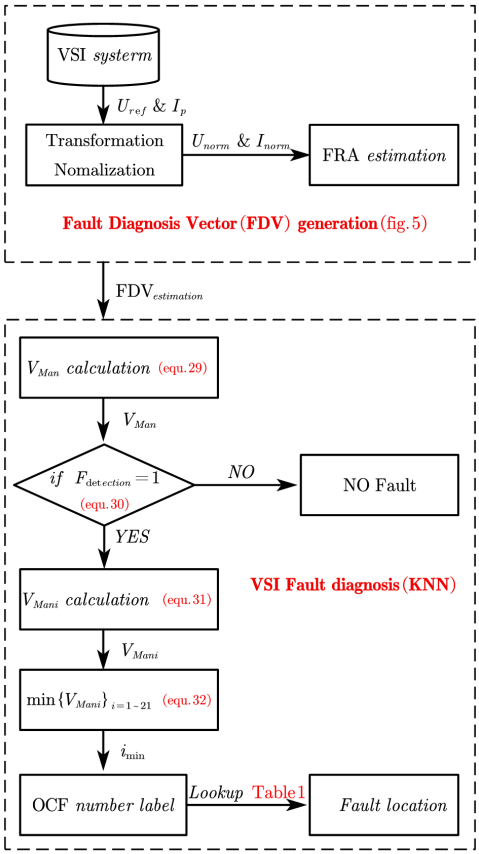

FIGURE 6. Flowchart of three-phase VSI diagnosis.

3) Fault location requires the calculation of the Manhattan distance value V_{Mani} between the FDV_{est} and the other 21 FDVs in the base matrix (Equ (31)), then use the fault location function $F_{location}$ (Equ (32)) to compare all V_{Mani} values to obtain the smallest V_{Mani} value, and the smallest V_{Mani} corresponding number i_{min} is the OCF number label.

4) Finally, the faulty switching device of the OCF can be located by lookuping Table 1 of OCF number label.

V. RESULT AND DISCUSSION

A. EXPERIMENT SETUP

An experimental inverter system, as shown in Fig. 7, is setup to validate the proposed fault diagnose scheme. This comprises an IGBT three-phase inverter cabinet with its associated hardware equipment, along with a dSPACE system. The dSPACE system includes DS1007, DS2002A/D Board and DS4004 I/O Board, current sensors and supporting software development tools for control, communication, fault simulation and fault diagnosis algorithm operation. The inverter cabinet contains 6 IGBTs and the corresponding dSPACE system interface; the main circuit can interact with the dSPACE system for real-time communication. The current sensors detect the values of the VSI three-phase currents, and these values are transmitted to the dSPACE

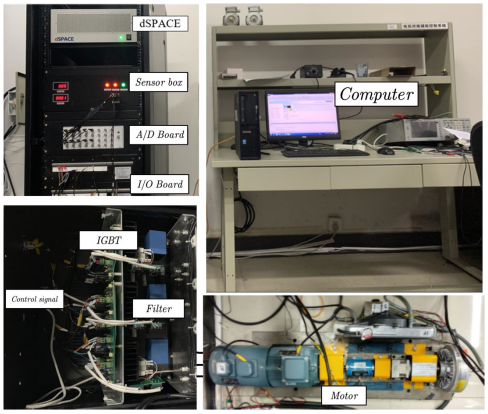

FIGURE 7. Experimental setup.

TABLE 2. Main parameters of the experimental setup.

Parameters	Symbol	Value
DC link voltage	V_{dc}	500v
Filter inductances	$L_aL_bL_c$	1.1mH
Filter Capacitors	$C_aC_bC_c$	50uF
Sample period	T_{sample}	5ms
Motor Rated power	P	7.5kW
Motor voltage (fundamental RMS)	U_{RMS}	380V
Motor current (fundamental RMS)	I_{RMS}	15.4A
Rated speed	n	1460rpm(continues)
Power factor	$cos\varphi$	0.86
Rated frequency	f	50.0Hz
Rated torque	T_e	48.96Nm
Efficiency (sine wave power supply)	η	0.93
Motor poles	p	4

system. The dSPACE system is connected to a computer, where fault detection and location can be performed using the diagnosis method described.

The main parameters of the inverter drive system are listed in Table 2. It should be noted that the machine drive is a variable load system, variations of the load and rotating speed are correlated. The experiments are performed to validate the model parameter-based fault diagnosis method at three rotor speeds. These are 1460 rpm, 1095 rpm and 730 rpm for load setting at 100% full power, 75% power and 50% power respectively.

B. ANALYSIS OF RESULTS

The experiments are firstly performed using three different sets of loads under three different speeds at normal operation conditions, hence three FDVs are estimated. Note the proposed fault diagnosis scheme must have the base matrix for the inverter drive system under test established, and it consists of two stages as shown in Fig. 6; namely, the inverter fault detection, and then the fault location identification.

1) FAULT DETECTION

Fig. 8 presents the three-phase current waveforms of VSI operating normally at speeds of 1460 rpm, 1095 rpm, and

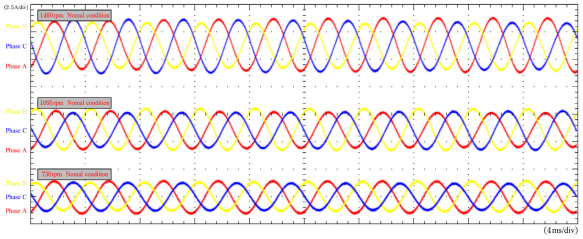

FIGURE 8. Experimental waveform of normal condition.

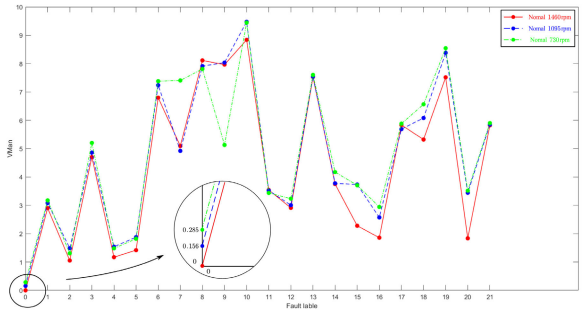

FIGURE 9. Detection of OCFs.

730 rpm. Three FDVs were obtained by subjecting the measured current values to FRA generation as illustrated in Fig. 6. The estimated three FDVs are applied to evaluate the corresponding V_{Man} according to equation (31). The results are displayed in Fig. 9. The X-axis gives the fault label numbers and the Y-axis is for the V_{Man} values used for fault diagnosis. As can be seen, for the normal condition, the three V_{Man} values obtained are all smaller than 1. However for the rest of 21 different fault cases, the V_{Man} values obtained corresponding to different loads are all greater than 1. It is evident that the method is effective in detecting fault free conditions under different load.

2) FAULT LOCATION IDENTIFICATION

According to the fault classification shown in Table 1, different types of faults are labeled to perform fault location identification. For single-switch OCF, for example, either T_1, or T_3, or T_5, the fault numbers are respectively 1, 3, 5 respectively in Table 1. Under each of these three fault cases, inverter phase currents are measured and their corresponding FDV_{est} are derived. They are used for fault detection first using equation (30). Then to locate the fault switches, equation (32) is applied, and the three V_{Man} are obtained.

Fig. 10 depicts the experimental waveform of three-phase currents in the VSI under the rated speed of 1460 rpm when faults T_1, T_3, and T_5 occur. The corresponding V_{Man} curves can be obtained using the methods presented in this paper, as shown in Fig. 11.

From the V_{Man} curves shown in Fig. 11, the values of those below 1 are fault cases with V_{Man} values precisely at the point corresponding to the faulty switch numbers. In Fig. 11,

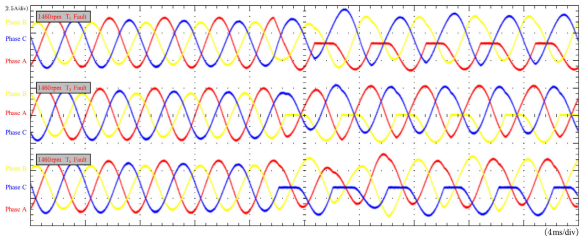

FIGURE 10. Experimental waveform of single-phase OCFs.

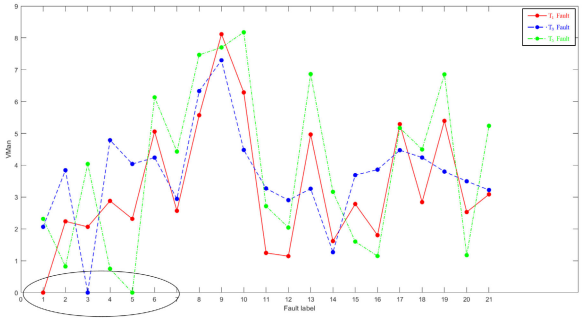

FIGURE 11. Fault location of single-phase OCFs.

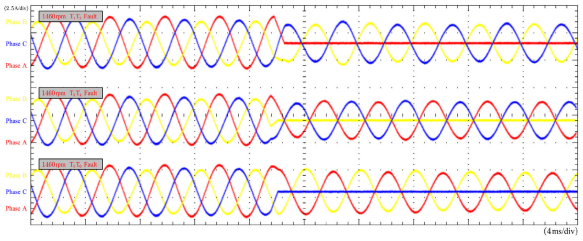

FIGURE 12. Experimental waveform of same phase double switch OCFs.

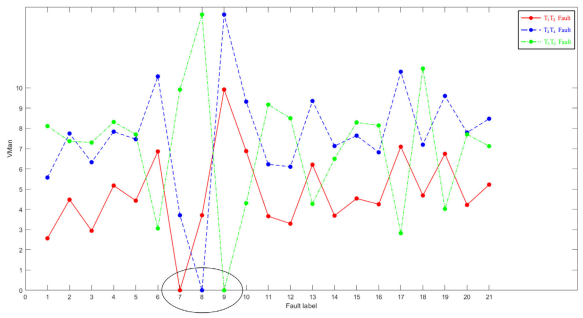

FIGURE 13. Fault location of heterogeneous double switch OCFs.

the red curve, which is for detecting T_1 fault, its minimum V_{Man} value is less than 1, and is located at point 1 on X-axis indicating that the faulty switch is T_1, and the fault location is successfully found. Similarly V_{Man} values at number 3 (blue) and 5 (green) are also smaller than 1, on the contrary V_{Man} at other 19 points are larger than 1, indicating clearly T_3 and T_5 are faulty.

Similarly, the method is applied to identify double switch faults, such as T_1-T_2, T_3-T_4, T_5-T_6, and the experimental

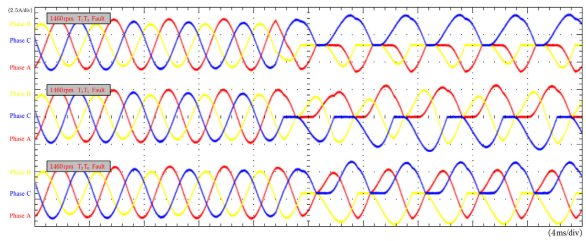

FIGURE 14. Experimental waveform of heterogeneous double switches.

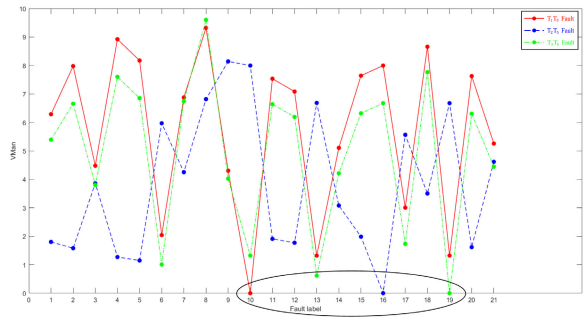

FIGURE 15. Fault location of heterogeneous double switch OCFs.

waveform plots and the corresponding V_{Man} results are shown separately in Fig. 12 and Fig. 13. V_{Man} values at numbers 7, 8, 9 are near zero, but above 1 at other case numbers. Thus faulty switches are located. For locating faults occurring simultaneous on two switches of different phases, for example, T_1-T_3, T_2-T_5, T_3-T_6, they correspond faults numbers are 10, 16, 19 respectively. The experimental waveform plot is as shown in Fig. 14. The V_{Man} results displayed in Fig. 15 show that very small V_{Man} values are observed at just these three case numbers, while the values are significantly larger for the other case numbers, therefore the fault locations are easily identified.

C. FAULT DIAGNOSIS UNDER VARIABLE LOADS

The proposed method is further validated for fault operation with different loads. For testing a single-phase single-switch OCF, switch T_4 is selected. For a single-phase double-switch fault, switches T_2-T_4 are chosen, and finally for a heterogeneous double-switch case, T_3-T_5 are considered.

The experimental waveform plots are shown in Fig 16, 18, and 20, respectively. The V_{Man} results are shown in Fig. 17, 19 and 21. The three curves in each figure represent, respectively, the V_{Man} variations for the corresponding faults at load speeds of 1460 rpm, 1095 rpm and 730 rpm. The lowest value of V_{Man} for all three localization curves shown in Fig. 17 is 4, indicating that the fault is located in the inverter switch corresponding to the label 4, which is T_4 switch. The fault location is accurately identified. The same analysis can be applied to check results depicted in both Fig. 19 and Fig. 21. In Fig. 19 three V_{Man} curves are displayed, their minimum V_{Man} all locate at x-axis point 8, which gives OCFs on T_3 and T_4 according to Table 1. V_{Man} variations for three

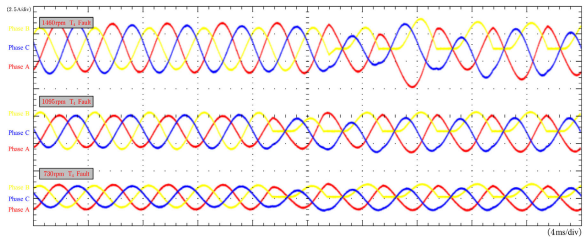

FIGURE 16. Experimental waveform of T_4 under different load.

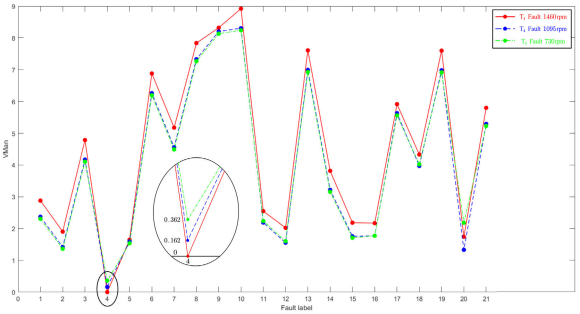

FIGURE 17. Fault location of T_4 under different load.

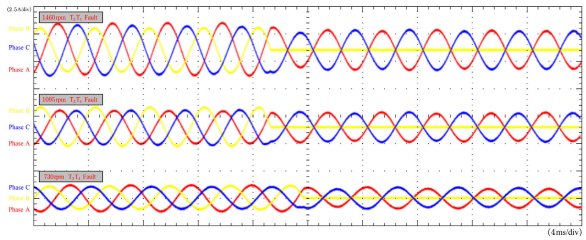

FIGURE 18. Experimental waveform of T_3T_4 under different load.

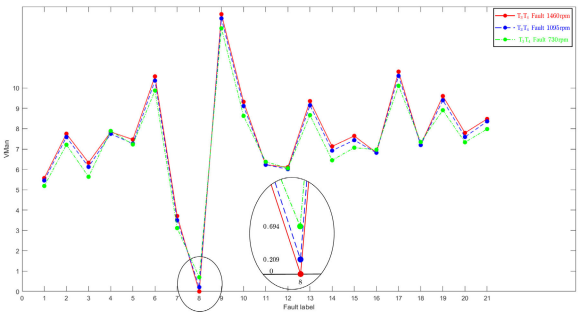

FIGURE 19. Fault location of T_3T_4 under different load.

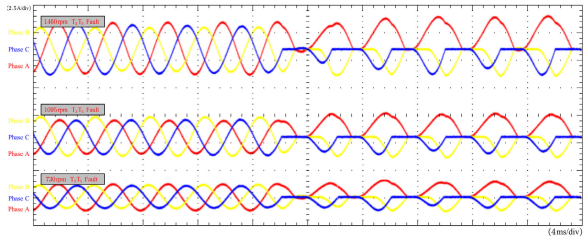

FIGURE 20. Experimental waveform of T_3T_5 under different load.

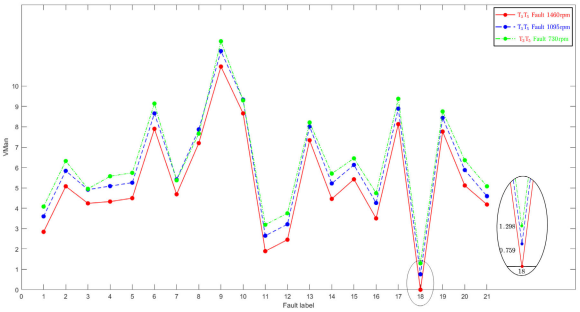

FIGURE 21. Fault location of T_3T_5 under different load.

different loads shown in Fig. 21 give the minimum values all at point 18, which presents OCFs occur at switches T_3 and T_5. These results confirm that the lowest points of V_{Man} curves for the same fault but with different loads fall correctly on the corresponding fault label. Thus the method based on V_{Man} can accurately locate the faulty switches and is not affected by the load variations.

D. DISCUSSION

The fault diagnosis method presented in this paper is based on a three-phase VSI model, which offers numerous advantages. Compared to traditional voltage-based diagnostic methods, the method does not require additional measurement and processing equipment, and it overcomes the drawback of current-based methods, which suffer from reduced accuracy during load variations. The method offers fast diagnosis and high reliability compared to fault diagnosis methods utilizing deep learning algorithms. It places less demand on computational resources, including memory and reduces computational complexity significantly. Additionally, the method is highly efficient, requiring minimal training and demonstrating excellent transferability. This sets it apart from numerous deep learning techniques, which typically demand extensive fault data for training purposes. It also requires fewer data samples due to the limited FDV variations after normalizing the 22 potential inverter conditions in the three-phase VSI. In the method, we apply the simplest K-Nearest Neighbors (KNN) algorithm, but the unique feature is that it relies on parameter model identification. After obtaining basic FDVs matix, we use KNN for fault diagnosis, and the FDV_{est} exhibits clear fault data characteristics, eliminating the need for further optimization of the KNN algorithm.

Generally, fault diagnosis methods based on Support Vector Machine (SVM) for inverters involve extracting fault information and then training and processing it using the SVM module. The SVM-based approach requires consideration of SVM optimization issues, as it may be affected by some disturbance data. In the proposed method for three-phase inverter fault diagnosis, the process is simple, and the diagnosis is precise.

However, the method has its limitations. Firstly, it relies on a linear three-phase VSI model. If the system exhibits high nonlinearity, parameter estimation may experience

significant variations, leading to reduced diagnostic accuracy. Furthermore, the method can be adapted for single-phase inverter fault diagnosis, but for multi-level inverter fault diagnosis, further research is needed. With an increase in the number of switches in multi-level inverters, the differences between multiple FDVs, as observed in the approach, may not be as pronounced, resulting in reduced diagnostic accuracy.

For future research plans, we will explore more efficient applications of the proposed method, such as enhancing the speed and accuracy of parameter estimation and assessing its applicability to various VSI systems.

VI. CONCLUSION

This paper has proposed a new model-based fault diagnosis method for three-phase inverters with variable loads. Based on the inverter current model, the Fast Recursive Algorithm(FRA) was applied to estimate the model parameters which vary under different switch OCF fault conditions. The diagnosis time for different types of OCFs is less than the phase current fundamental period. The whole diagnosis process consists of fault detection and location which are implemented by a simple decision making function. An experimental inverter drive platform with different loads was tested to validate the effectiveness of the proposed method. The experimental results of fault detection and location identification verify that the proposed diagnosis method can accurately detect and locate single switch and double switch OCFs. The diagnosis results for the same fault under different loads showed that the method is robust against load variations.

REFERENCES

[1] A. M. Hava and E. Un, "Performance analysis of reduced common-mode voltage PWM methods and comparison with standard PWM methods for three-phase voltage-source inverters," *IEEE Trans. Power Electron.*, vol. 24, no. 1, pp. 241–252, Jan. 2009.

[2] M. Alavi, D. Wang, and M. Luo, "Short-circuit fault diagnosis for three-phase inverters based on voltage-space patterns," *IEEE Trans. Ind. Electron.*, vol. 61, no. 10, pp. 5558–5569, Oct. 2014.

[3] B. A. Welchko, M. B. de Rossiter Correa, and T. A. Lipo, "A three-level MOSFET inverter for low-power drives," *IEEE Trans. Ind. Electron.*, vol. 51, no. 3, pp. 669–674, Jun. 2004.

[4] B. Baodong and C. Dezhi, "Inverter IGBT loss analysis and calculation," in *Proc. IEEE Int. Conf. Ind. Technol. (ICIT)*, Feb. 2013, pp. 563–569.

[5] X. Ding, M. Du, C. Duan, H. Guo, R. Xiong, J. Xu, J. Cheng, and P. C. K. Luk, "Analytical and experimental evaluation of SiC-inverter nonlinearities for traction drives used in electric vehicles," *IEEE Trans. Veh. Technol.*, vol. 67, no. 1, pp. 146–159, Jan. 2018.

[6] Y. Song and B. Wang, "Survey on reliability of power electronic systems," *IEEE Trans. Power Electron.*, vol. 28, no. 1, pp. 591–604, Jan. 2013.

[7] M. A. Masrur, Z. Chen, and Y. Murphey, "Intelligent diagnosis of open and short circuit faults in electric drive inverters for real-time applications," *IET Power Electron.*, vol. 3, no. 2, pp. 279–291, 2010.

[8] S. Yang, A. Bryant, P. Mawby, D. Xiang, L. Ran, and P. Tavner, "An industry-based survey of reliability in power electronic converters," *IEEE Trans. Ind. Appl.*, vol. 47, no. 3, pp. 1441–1451, May 2011.

[9] S. Karimi, A. Gaillard, P. Poure, and S. Saadate, "FPGA-based real-time power converter failure diagnosis for wind energy conversion systems," *IEEE Trans. Ind. Electron.*, vol. 55, no. 12, pp. 4299–4308, Dec. 2008.

[10] Z. Li, H. Ma, Z. Bai, Y. Wang, and B. Wang, "Fast transistor open-circuit faults diagnosis in grid-tied three-phase VSIs based on average bridge arm pole-to-pole voltages and error-adaptive thresholds," *IEEE Trans. Power Electron.*, vol. 33, no. 9, pp. 8040–8051, Sep. 2018.

[11] O.-S. Yu, N.-J. Park, and D.-S. Hyun, "A novel fault detection scheme for voltage fed PWM inverter," in *Proc. 32nd Annu. Conf. IEEE Ind. Electron. (IECON)*, Nov. 2006, pp. 2654–2659.

[12] Q. T. An, L. Sun, and L. Z. Sun, "Hardware-circuit-based diagnosis method for open-switch faults in inverters," *Electron. Lett.*, vol. 49, no. 17, pp. 1089–1091, Aug. 2013.

[13] F. Wu and J. Zhao, "A real-time multiple open-circuit fault diagnosis method in voltage-source-inverter fed vector controlled drives," *IEEE Trans. Power Electron.*, vol. 31, no. 2, pp. 1425–1437, Feb. 2016.

[14] X. Pei, "Open-circuit fault diagnosis based on the filter inductor voltage for single- and three-phase inverters," in *Proc. Int. Power, Electron. Mater. Eng. Conf.*, 2015, pp. 327–333.

[15] C. Shu, C. Ya-Ting, Y. Tian-Jian, and W. Xun, "A novel diagnostic technique for open-circuited faults of inverters based on output line-to-line voltage model," *IEEE Trans. Ind. Electron.*, vol. 63, no. 7, pp. 4412–4421, Jul. 2016.

[16] Y. Wang, Z. Li, M. Xu, and H. Ma, "A comparative study of two diagnostic methods based on the switching voltage pattern for IGBT open-circuit faults in voltage-source inverters," *J. Power Electron.*, vol. 16, no. 3, pp. 1087–1096, May 2016.

[17] H. Wei, Y. Zhang, L. Yu, M. Zhang, and K. Teffah, "A new diagnostic algorithm for multiple IGBTs open circuit faults by the phase currents for power inverter in electric vehicles," *Energies*, vol. 11, no. 6, p. 1508, Jun. 2018.

[18] R. Selvaraj, K. Desingu, T. R. Chelliah, D. Khare, and C. Bharatiraja, "Fault tolerant operation of parallel-connected 3L-neutral-point clamped back-to-back converters serving to large hydro-generating units," *IEEE Trans. Ind. Appl.*, vol. 54, no. 5, pp. 5429–5443, Sep. 2018.

[19] A. Shahin, J.-P. Martin, and S. Pierfederici, "Zero-sequence current based diagnostic method for open-switch fault detection in parallel inverters system," *IEEE Trans. Power Electron.*, vol. 34, no. 4, pp. 3750–3764, Apr. 2019.

[20] M. S. Shadlu, "Fault detection and diagnosis in voltage source inverters using principle component analysis," in *Proc. IEEE 4th Int. Conf. Knowl.-Based Eng. Innov. (KBEI)*, Dec. 2017, pp. 509–515.

[21] Y. Mei and H. Yuan, "A novel open-circuit fault diagnosis method for voltage source inverter," in *Proc. IEEE Int. Power Electron. Appl. Conf. Expo. (PEAC)*, Nov. 2018, pp. 1–6.

[22] W. Sleszynski, J. Nieznanski, and A. Cichowski, "Open-transistor fault diagnostics in voltage-source inverters by analyzing the load currents," *IEEE Trans. Ind. Electron.*, vol. 56, no. 11, pp. 4681–4688, Nov. 2009.

[23] S. Valipour, S. S. Moosavi, D. A. Khaburi, and A. Djerdir, "An open-circuit fault detection method using wavelet transform for cascaded H-bridge multilevel inverter," in *Proc. IEEE Vehicle Power Propuls. Conf. (VPPC)*, Dec. 2017, pp. 1–5.

[24] I. Abari, M. Hamouda, and J. B. H. Slama, "Three-level NPC inverter fault diagnosis using wavelet packet transform and statistical analysis of the emitted near-field," in *Proc. 12th Int. Renew. Energy Congr. (IREC)*, Oct. 2021, pp. 1–5.

[25] I. Abari, M. Hamouda, J. B. H. Slama, and K. Al-Haddad, "Single switch open-circuit fault detection for three-level NPC inverter using conducted emissions signature," in *Proc. 44th Annu. Conf. IEEE Ind. Electron. Soc. (IECON)*, Oct. 2018, pp. 1489–1494.

[26] I. Abari, M. Hamouda, and J. B. H. Slama, "Open-switch fault detection in three-phase symmetrical cascaded multilevel inverter using conducted disturbances," in *Proc. 15th Int. Multi-Conf. Syst., Signals Devices (SSD)*, Mar. 2018, pp. 77–82.

[27] Q.-T. An, L.-Z. Sun, K. Zhao, and L. Sun, "Switching function model-based fast-diagnostic method of open-switch faults in inverters without sensors," *IEEE Trans. Power Electron.*, vol. 26, no. 1, pp. 119–126, Jan. 2011.

[28] Q.-T. An, L. Sun, and L.-Z. Sun, "Current residual vector-based open-switch fault diagnosis of inverters in PMSM drive systems," *IEEE Trans. Power Electron.*, vol. 30, no. 5, pp. 2814–2827, May 2015.

[29] J. Zhang, J. Zhao, D. Zhou, and C. Huang, "High-performance fault diagnosis in PWM voltage-source inverters for vector-controlled induction motor drives," *IEEE Trans. Power Electron.*, vol. 29, no. 11, pp. 6087–6099, Nov. 2014.

[30] S. S. Moosavi, A. Kazemi, and H. Akbari, "A comparison of various open-circuit fault detection methods in the IGBT-based DC/AC inverter used in electric vehicle," *Eng. Failure Anal.*, vol. 96, pp. 223–235, Feb. 2019.

[31] T. Jiang, Y. Wang, and Z. Li, "Fault diagnosis of three-phase inverter based on CEEMDAN and GWO-SVM," in *Proc. Chin. Autom. Congr. (CAC)*, Nov. 2020, pp. 2362–2368.
[32] M. Ali, Z. Din, E. Solomin, K. M. Cheema, A. H. Milyani, and Z. Che, "Open switch fault diagnosis of cascade H-bridge multi-level inverter in distributed power generators by machine learning algorithms," *Energy Rep.*, vol. 7, pp. 8929–8942, Nov. 2021.
[33] W. Yuan, Z. Li, Y. He, R. Cheng, L. Lu, and Y. Ruan, "Open-circuit fault diagnosis of NPC inverter based on improved 1-D CNN network," *IEEE Trans. Instrum. Meas.*, vol. 71, pp. 1–11, 2022.
[34] K. Li, J.-X. Peng, and G. W. Irwin, "A fast nonlinear model identification method," *IEEE Trans. Autom. Control*, vol. 50, no. 8, pp. 1211–1216, Aug. 2005.
[35] S. Zhang, X. Li, M. Zong, X. Zhu, and R. Wang, "Efficient kNN classification with different numbers of nearest neighbors," *IEEE Trans. Neural Netw. Learn. Syst.*, vol. 29, no. 5, pp. 1774–1785, May 2018.

YU LUO received the B.E. degree in electrical automation and the M.S. degree in electrical engineering from the Changsha University of Science and Technology, China, in 2013 and 2016, respectively. He is currently pursuing the Ph.D. degree with the School of Transportation Engineering, Central South University, China.

His research interests include fault diagnosis, fault tolerant control of power electronic converters, train control, and traction electric drives.

LI ZHANG (Senior Member, IEEE) received the Ph.D. degree from Oxford University, U.K. She was a Research Fellow with Oxford University. She was also a Lecturer with the University of Bradford. She is currently a Senior Lecturer with the School of Electronic and Electrical Engineering, University of Leeds, U.K. She has been an Adjunct Professor with Chongqing University, China, since 2006, and a Joint Grant holder of China State Natural Science Foundation Fund, entitled "Analysis and Research on the Hot Spot Effect and It's Control Method of Photovoltaic System." She has authored or coauthored three books on power converter circuits and wind power electricity generation; and more than 130 technical papers in the fields of power electronics, renewable power generation systems, and wind generator control. She is an Associate Editor of IEEE TRANSACTIONS ON POWER ELECTRONICS and was an Associate Editor of *IET Proceedings on Power Electronics*, from 2014 to 2017.

CHUNYANG CHEN was born in Nanling, China, in 1962. He received the B.E. degree in electric locomotive from Southwest Jiaotong University, the master's degree from Hunan University, and the Ph.D. degree from Beijing Jiaotong University. He was the Deputy Director of the Science and Technology Department, Ministry of Railways; and the President of Southwest Jiaotong University. Currently, he is the Vice President of Central South University. His research interests include the electric locomotive and intelligent transportation systems.

KANG LI (Senior Member, IEEE) received the B.Sc. degree in industrial automation from Xiangtan University, Hunan, China, in 1989, the M.Sc. degree in control theory and applications from the Harbin Institute of Technology, Harbin, China, in 1992, the Ph.D. degree in control theory and applications from Shanghai Jiaotong University, Shanghai, China, in 1995, and the D.Sc. degree in engineering from Queen's University Belfast, U.K., in 2015. He currently holds the Chair of smart energy systems with the University of Leeds, U.K. His research interests cover nonlinear system modeling, identification, and control; machine learning, with substantial applications to energy and power systems; transport decarbonization; and energy management in energy intensive manufacturing processes.

TIANJIAN YU received the Ph.D. degree in traffic equipment and information engineering from Central South University, Changsha, China, in 2017. Since 2014, he has been a Visiting Ph.D. Student with the University of Pittsburgh, PA, USA. He is currently a Researcher with the School of Traffic and Transportation Engineering, Central South University. His research interests include fault diagnosis of traffic equipment, in particular on bearings and inverters.

KAIDI LI was born in Nanning, China, in 1992. He received the B.E. degree in electrical engineering from the Changsha University of Science and Technology, China, in 2013, and the M.S. degree in electrical engineering and the Ph.D. degree in traffic equipment and information engineering from Central South University (CSU), China, in 2016 and 2019, respectively.

He is currently with the Shenzhen Metro Group Company Ltd., Shenzhen, China. His research areas include fault diagnosis and fault tolerant control of power electronic converters.